

Calculation of Relative Hydration Free Energy Differences for Heteroaromatic Compounds: Use in the Design of Adenosine Deaminase and Cytidine Deaminase Inhibitors

Mark D. Erion* and M. Rami Reddy*

Contribution from Metabasis Therapeutics, Inc., 9390 Towne Centre Drive, San Diego, California 92121

Received August 18, 1997

Abstract: Heteroaromatic compounds frequently undergo reversible covalent hydration in aqueous solution with the extent of hydration dependent on the heterocycle and its substituents. Using a combined quantum mechanical and thermodynamic cycle perturbation (TCP) approach, relative hydration free energy differences ($\Delta\Delta G_{\text{hyd}}$) were calculated for a variety of pteridine, quinazoline, pyrimidine, and purine analogues. Good agreement with experimental data was obtained for heteroaromatic compounds exhibiting a wide range of hydration equilibrium constants (10^{-6} – 10^3). Differences in hydration were attributed to a multitude of molecular factors including both electronic and steric effects. Differences in the resonance energy lost during hydration of the heteroaromatic ring accounted for the 10^7 -fold greater hydration of pteridine relative to 9-methylpurine ($\Delta\Delta G_{\text{hyd}}(\text{exp}) \approx -8.8$ kcal/mol; $\Delta\Delta G_{\text{hyd}}(\text{calc}) = -9.3$ kcal/mol). An analysis of purine riboside and its 8-aza analogue showed that the 400-fold greater adenosine deaminase (ADA) inhibitor potency exhibited by the 8-aza analogue is accurately calculated by summing the hydration free energy difference with the relative binding free energy difference for the corresponding hydrated species. The greater inhibitor potency was attributed to increased hydration since hydration of 8-aza-9-methylpurine was strongly favored over 9-methylpurine ($\Delta\Delta G_{\text{hyd}} = -7.1$ kcal/mol), whereas the relative binding free energy calculated using the TCP method and the murine ADA structure favored the purine riboside hydrate ($\Delta\Delta G_{\text{bind}} = 3.1 \pm 0.7$ kcal/mol). Increased desolvation costs for the 8-aza analogue and an unfavorable electrostatic interaction between the 8-nitrogen and Asp296 accounted for the loss in binding affinity. The combined results gave an apparent inhibition constant for the 8-aza analogue similar to the experimental value and demonstrated the potential importance of hydration free energy calculations in drug design.

Introduction

Addition of water to a double or triple bond is the first step in a variety of enzyme-catalyzed reactions. Examples include both hydrolytic reactions, such as those catalyzed by proteases, esterases, and deaminases and nonhydrolytic reactions such as the reactions catalyzed by some dehydrogenases and oxidases. In each case, efficient catalysis occurs by stabilization of a transition state structure that resembles the tetrahedral hydrate intermediate.¹ Accordingly, compounds that form a covalent hydrate in aqueous solution often produce potent enzyme inhibition through mimicry of the transition state structure.² For example, zinc metalloproteases and aspartyl proteases are inhibited by trifluoromethyl ketones but not methyl ketones since inhibition is via the hydrated species and trifluoromethyl ketones hydrate to a much greater extent.³ The extent of hydration, as characterized by the equilibrium constant, is therefore an important parameter that not only can affect the chemical and spectral properties of molecules in aqueous solution but can also play an important role in defining their biological activity. Consequently, efforts are ongoing to identify methods for predicting the equilibrium constant and the molecular factors controlling hydration.

Carbonyl-containing compounds are the most studied class of compounds because of their propensity to hydrate⁴ and relative structural simplicity. Methods for the calculation of absolute hydration free energies using quantum mechanics were reported,⁵ and, in some cases, reasonable agreement was obtained between the calculated and experimental results.^{5a} In other cases, however, significant deviations were noted and ascribed to several possible factors, including the level of quantum mechanical theory used in the calculations and the failure to include solvation free energies.^{5b} Recently, we reported a method that uses both quantum mechanical and free energy perturbation methods for calculating relative changes in the hydration free energies between two similar molecules.⁶ Calculated results were in good agreement with experimental data over a large set of carbonyl-containing compounds. Greater accuracy was achieved for relative free energy differences compared to absolute free energies presumably due to the cancellation of systematic errors and to increased convergence in the solvation free energy calculation. Importantly, the results were in good agreement with experimental results even at lower levels of quantum mechanical theory. Calculation of relative

* Correspondence may be addressed to either author. E-mail: erion@mbasis.com or reddy@mbasis.com. Fax: 619-622-5545.

(1) Wolfenden, R. *Annu. Rev. Biophys. Bioeng.* **1976**, *5*, 271–306.

(2) Kati, W. M.; Wolfenden, R. *Science* **1989**, *243*, 1591–1593.

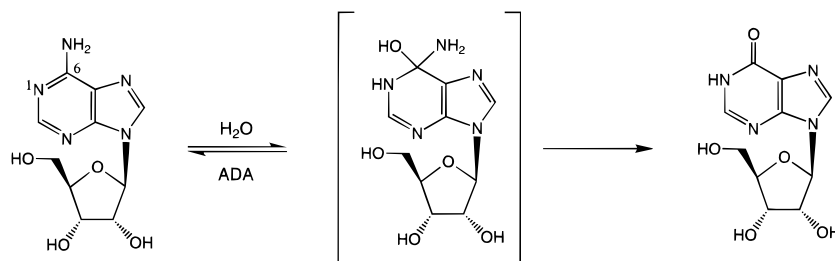
(3) Gelb, M. H.; Svaren, J. P.; Abeles, R. H. *Biochemistry* **1985**, *24*, 1813–1817.

(4) Bell, R. P. *Adv. Phys. Org. Chem.* **1966**, *4*, 1–29.

(5) (a) Wiberg, K. B.; Morgan, K. M.; Maltz, H. *J. Am. Chem. Soc.* **1994**, *116*, 11067–11077. (b) Henke, S. L.; Hada, C. M.; Morgan, K. M.; Wiberg, K. B.; Wasserman, H. H. *J. Org. Chem.* **1993**, *58*, 2830–2839.

(6) Erion, M. D.; Reddy, M. R. *J. Comput. Chem.* **1995**, *12*, 1513–1521.

Scheme 1



free energy differences using this method was therefore considered more useful than previous methods for analysis of medium-sized molecules and drug design.

Heteroaromatic compounds represent another class of organic compounds that undergo covalent hydration in aqueous solution. Numerous studies have been conducted since the reaction was first observed in 1951 detailing the hydration kinetics for a large number of structurally diverse heteroaromatic compounds.⁷ More recently, a variety of enzymes have been identified that catalyze the hydration of heteroaromatic compounds or utilize the hydrated species as the substrate. Some of these enzymes represent well-recognized drug targets. For example, adenosine deaminase⁸ and cytidine deaminase⁹ catalyze the deamination of heteroaromatic compounds via an unstable hydrated intermediate (Scheme 1). Both enzymes are of interest to the pharmaceutical industry based on their potential as targets for anti-ischemic and anti-cancer agents, respectively. IMP dehydrogenase and xanthine oxidase are two other drug targets that purportedly use covalent hydration as a key step in their catalytic mechanism. Heteroaromatic hydration has also been identified as an essential element in the inhibitory mechanisms of several highly potent enzyme inhibitors.^{2,10} Accordingly, factors controlling heteroaromatic hydration and methods used to accurately predict the extent of hydration are expected to aid drug design. Described herein is the first theoretical investigation of the heteroaromatic hydration reaction. In this study, relative

hydration free energy differences were calculated for a variety of pteridine, quinazoline, purine, and pyrimidine analogues. Factors controlling the extent of hydration were also identified and incorporated into the design and analysis of potential adenosine deaminase and cytidine deaminase inhibitors.

Methodology

The reversible addition of water to molecule A is described by the equilibrium constant, K_{eq}^A (eq 1) and associated hydration free energy ΔG_{hyd}^A (eq 2).

$$K_{\text{eq}}^A = [A - \text{H}_2\text{O}]/[A][\text{H}_2\text{O}] \quad (1)$$

$$\Delta G_{\text{hyd}}^A = -RT \ln K_{\text{eq}}^A \quad (2)$$

The hydration free energy difference for molecules A and B is given by eqs 3 and 4

$$\Delta \Delta G_{\text{hyd}}^{\text{AB}} = \Delta G_{\text{hyd}}^{\text{B}} - \Delta G_{\text{hyd}}^{\text{A}} \quad (3)$$

$$\Delta \Delta G_{\text{hyd}}^{\text{AB}} = \Delta \Delta G_{\text{gas}}^{\text{AB}} + \Delta \Delta \Delta G_{\text{sol}}^{\text{AB}} \quad (4)$$

where $\Delta \Delta G_{\text{gas}}^{\text{AB}}$ and $\Delta \Delta \Delta G_{\text{sol}}^{\text{AB}}$ are the relative differences in gas-phase quantum mechanical free energy and solvation free energy, respectively.

Gas-Phase Free Energies. The gas-phase free energies ($\Delta \Delta G_{\text{gas}}$) were calculated using energies obtained from ab initio quantum mechanical calculations at the HF/6-31G** basis set level¹¹ on fully geometry optimized anhydrous and hydrated heteroaromatic compounds. The calculated energy represents the energy for the global energy minimum structure. The harmonic frequencies for each molecule were calculated at the HF/6-31G** basis set level and used to calculate the zero-point energies and the thermal contributions to the vibrational energies.

Solvation Free Energies. Molecular dynamics (MD) simulations in conjunction with the thermodynamic cycle perturbation (TCP) approach were used to calculate relative solvation free energies between two similar molecules.¹² $\Delta \Delta \Delta G_{\text{sol}}$ was calculated using eq 5, where

$$\Delta \Delta \Delta G_{\text{sol}} = \Delta \Delta G_{\text{sol}}(\text{products}) - \Delta \Delta G_{\text{sol}}(\text{reactants}) \quad (5)$$

$\Delta \Delta G_{\text{sol}}(\text{products})$ and $\Delta \Delta G_{\text{sol}}(\text{reactants})$ are the relative solvation free energy differences between the two products and two reactants of the two hydration reactions, respectively. The

(7) (a) Albert, A. *Adv. Heterocycl. Chem.* **1976**, *20*, 117–143. (b) Albert, A.; Armarego, W. L. F. *Adv. Heterocycl. Chem.* **1965**, *4*, 1–42. (c) Perrin, D. D. *Adv. Heterocycl. Chem.* **1965**, *4*, 43–73.

(8) (a) Wolfenden, R.; Kaufman, J.; Macon, J. B. *Biochemistry* **1969**, *8*, 2412–2415. (b) Kati, W. M.; Acheson, S. A.; Wolfenden, R. *Biochemistry* **1992**, *31*, 7356–7366.

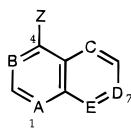
(9) (a) Cohen, R. M.; Wolfenden, R. *J. Biol. Chem.* **1971**, *246*, 7561–7565. (b) Frick, L.; Yang, C.; Marquez, V. E.; Wolfenden, R. *Biochemistry* **1989**, *28*, 9423–9430.

(10) Jones, W.; Kurz, L. C.; Wolfenden, R. *Biochemistry* **1989**, *28*, 1242–1247.

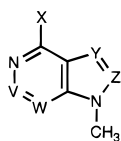
(11) (a) Foresman, J. B.; Frisch, A. *Exploring Chemistry with Electronic Structure Methods: A Guide to Using Gaussian*; Gaussian, Inc.: Pittsburgh, PA, 1993. (b) Hehre, W. J.; Radom, L.; Schleyer, P. v. R.; Pople, J. A. *Ab Initio Molecular Orbital Theory*; Wiley: New York, 1986. (c) Frisch, M. J.; Head-Gordon, M.; Schlegel, H. B.; Raghavachari, K.; Binkley, J. S.; Gonzalez, C.; Defrees, D. J.; Fox, D. J.; Whiteside, R. J.; Seeger, R.; Melius, C. F.; Baker, J.; Martin, R.; Kahn, L. R.; Stewart, J. J. P.; Fluder, E. M.; Topiol, S.; Pople, J. A. *Gaussian92*; Gaussian, Inc.: Pittsburgh, PA, 1992.

(12) (a) Zwanzig, R. W. *J. Chem. Phys.* **1954**, *22*, 1420–1426. (b) Tembe, B. L.; McCammon, J. A. *Comput. Chem.* **1982**, *8*, 281–283. (c) Beveridge, D. L.; DiCapua, F. M. *Annu. Rev. Biophys. Biophys. Chem.* **1989**, *18*, 431–492. (d) Van Gunsteren, W. F.; Weiner, P. K. *Computer Simulation of Biomolecular Systems*; ESCOM Science: Leiden, Netherlands, 1989. (e) *Molecular Dynamics and Protein Structure*; Hermans, J., Ed.; Polycrystal: West Springs, IL, 1985. (f) Reddy, M. R.; Bacquet, R. J.; Varney, M. D. *J. Chim. Phys.* **1991**, *88*, 2605–2615. (g) Jorgensen, W. L.; Briggs, J. M. *J. Am. Chem. Soc.* **1989**, *111*, 4190–4197. (h) Nagy, P. I.; Durant, G. J.; Smith, D. A. *J. Am. Chem. Soc.* **1993**, *115*, 2912–2922. (i) Bash, P. A.; Singh, U. C.; Brown, F. K.; Langridge, R.; Kollman, P. A. *Science* **1987**, *235*, 574–575. (j) Cieplak, P.; Bash, P.; Singh, U. C.; Kollman, P. A. *J. Am. Chem. Soc.* **1987**, *109*, 6283–6289. (k) Reddy, M. R.; Viswanadhan, V. N.; Weinstein, J. N. *Proc. Natl. Acad. Sci. U.S.A.* **1991**, *88*, 10287–10291.

(13) (a) Weiner, S. J.; Kollman, P. A.; Case, D. A.; Singh, U. C.; Ghio, C.; Alagoha, G.; Profeta, S., Jr.; Weiner, P. K. *J. Am. Chem. Soc.* **1984**, *106*, 765–784. (b) Singh, U. C.; Weiner, P. K.; Caldwell, J. K.; Kollman, P. A. AMBER Version 3.3; University of California at San Francisco: San Francisco, CA, 1992. (c) Singh, U. C. *Proc. Natl. Acad. Sci. U.S.A.* **1988**, *85*, 4280–4284. (d) Reddy, M. R.; Bacquet, R. J.; Zichi, D.; Mathews, D. A.; Welsh, K. M.; Jones, T. R.; Freer, S. *J. Am. Chem. Soc.* **1992**, *114*, 4, 10117–10122. (e) Singh, U. C.; Benkovic, S. J. *Proc. Natl. Acad. Sci. U.S.A.* **1988**, *85*, 9519–9523.

Table 1. Azanaphthalene Compounds

compd	A	B	C	D	E	Z	hydration site
1	N	N	N	CH	N	H	4
2	N	N	CH	CH	N	H	4
3	N	N	N	CH	CH	H	4
4	N	N	CH	N	CH	H	4
5	N	N	CH	CH	CH	H	4
6	N	N	N	N	N	H	4
7	CH	N	N	CH	N	H	7
8	CH	HN	N	CH	N	H	7
9a	N	N	N	CH	N	CH ₃	4
9b	N	N	N	CH	N	CH ₃	7
10a	N	N	N	CH	N	CF ₃	4
10b	N	N	N	CH	N	CF ₃	7

Table 2. Purine Analogues

compd	X	Y	Z	W	V
11	H	N	CH	N	CH
12	H	N	N	N	CH
13	H	N	CH	N	N
14	H	N	CH	CH	CH
15	H	CH	CH	N	CH
16	CF ₃	N	CH	N	CH
17	F	N	CH	N	CH
18	H	N	CH	N	CF
19	H	N	CF	N	CH

calculations were carried out using MD simulations and the window method implemented in the AMBER program.¹³ The computational details for both the quantum mechanical and TCP studies using molecular dynamics simulations are described elsewhere.⁶ The TCP calculations used a single topology for all mutations except for the mutation of 9-methylpurine (**11**) to peridine (**1**), which used the thread methodology due to significant structural dissimilarity.^{6,13e}

Binding Free Energies. The TCP approach was used to calculate the relative binding free energy difference between 1,6-double bond hydrates of purine riboside and 8-azapurine riboside with adenosine deaminase (ADA). The X-ray structure of murine adenosine deaminase complexed with (6R)-6-hydroxy-1,6-dihydropurine riboside (HPR) (pdb file name: 2ADA)¹⁴ provided the initial atomic coordinates used to generate the computer model and conduct the energy calculations. All molecular dynamics, molecular mechanics, and TCP calculations were carried out with the AMBER program using an all atom force field and SPC/E potentials¹⁵ to describe water interactions. Atomic charges and parameters for the standard residues were taken from the AMBER database. Partial atomic charges for nonstandard residues were obtained using CHELPG¹⁶ to fit the charges to the quantum mechanical electrostatic potential

(14) (a) Wilson, D. K.; Rudolph, F. B.; Quioco, F. A. *Science* **1991**, 252, 1278–1284. (b) Sharff, A. J.; Wilson, D. K.; Chang, Z.; Quioco, F. A. *J. Mol. Biol.* **1992**, 226, 917–921.

(15) (a) Berendsen, H. J. C.; Grigera, J. R.; Straatsma, T. P. *J. Phys. Chem.* **1987**, 91, 6269–6271. (b) Reddy, M. R.; Berkowitz, M. *Chem. Phys. Lett.* **1989**, 155, 173–176.

(16) Chirlian, L. E.; Francl, M. M. *J. Comput. Chem.* **1987**, 8, 894–905.

computed from ab initio 6-31G** wave functions calculated with Gaussian94.¹¹ All equilibrium bond lengths, bond angles, and dihedral angles for nonstandard residues were obtained from ab initio optimized geometries at the 6-31G** basis set level. Missing force field parameters were estimated from similar chemical species within the AMBER database.

Aqueous phase dynamics simulations were carried out in a rectangular box (40.1 Å × 34.9 Å × 34.5 Å) using periodic boundary conditions in all directions. The solute was solvated with 1602 SPC/E water^{15b} molecules using the AMBER box option, and all water molecules located less than 2.5 Å or greater than 15.0 Å from a solute atom were removed. The initial coordinates of HPR were obtained from the X-ray structure of the ADA-HPR complex. Newton's equations of motion for all the atoms were solved using the Verlet algorithm¹⁷ with a 1 fs time step and SHAKE for constraining all bond lengths.¹⁸ Constant temperature (N, P & T ensemble) was maintained by velocity scaling all atoms in the system. Nonbonded interaction energies were calculated using a 15.0 Å residue based cutoff.

Protein complex simulations were carried out using the ADA-HPR complex. Missing polar hydrogen atoms were added to protein residues in an orientation consistent with the crystallographic position of each heteroatom and its environment. The charge on the zinc ion was determined using the 3-21G* wave function calculated for zinc coordinated with residues present in the ADA-HPR complex. Each residue was capped with an acetyl group at the N-terminus and an NH₂ at the C-terminus. The calculated charge on zinc was +1.2 e, whereas the net charge on histidines 15, 17, and 214 was +0.2 e each and on the aspartic acid, Asp295, was −0.8 e. Thus, the net charge on the zinc complex was +1 e. Virtual bonds between zinc and the atoms which coordinate to the zinc ion (His15, NE2; His17, NE2; His214, NE2; Asp295, O2; HPR, O6) were added using the LINK module of the AMBER program in order to provide necessary atomic constraints prior to energy minimization and MD simulations. The complex was immersed in a 20.0 Å radius sphere of SPC/E water centered around the mutating group and subjected to a half-harmonic restraint near the boundary to prevent evaporation. During the simulation, all atoms of the protein were fixed beyond 20.0 Å. All nonbonded interactions involving the inhibitors and the charged residues of the protein were computed with an infinite cutoff, whereas a 15.0 Å nonbonded residue based cutoff was used for all other residues of the system. The algorithm for the complex simulation was identical to the solvent simulation except for the absence of periodic boundary conditions.

Free energy calculations were carried out after the solvated inhibitor and the ADA-inhibitor complex were energy minimized and subjected to a 20 ps preequilibration step using molecular dynamics. Energy minimization was accomplished using the AMBER force field and 500 steps of steepest descent followed by 2000 steps of conjugate gradient (RMS < 0.5 Å). Free energies were calculated using the TCP methodology. Accordingly, the free energy change for converting the reactant (S1) into the product (S2) was computed by slowly perturbing the Hamiltonian of S1 into S2 and summing the incremental free energy changes for a series of equally spaced nonphysical states (λ_i) that lie along a path linking the initial ($\lambda = 0$) and final ($\lambda = 1$) states. A total of 51 windows were used with each window comprising 2.5 ps of equilibration and 5 ps of data collection. The relative solvation free energy change for

(17) Verlet, L. *Phys. Rev.* **1967**, 159, 98–103.

(18) Ryckaert, J. P.; Ciccotti, G.; Berendsen, H. J. C. *J. Comput. Phys.* **1977**, 23, 327–341.

Table 3. Ab Initio Results

compd	$E(\text{HF})^a$	$E(0)^b$	$\Delta E(v)^b$	TS^b
1R	-447.333 56	68.065	1.863	23.432
1P	-523.361 00	87.102	2.969	25.984
2R	-431.348 43	75.890	1.953	23.589
2P	-507.373 83	95.026	3.053	26.211
3R	-431.348 80	75.924	1.943	23.558
3P	-507.375 03	94.997	3.051	26.116
4R	-431.343 86	75.893	1.965	23.612
4P	-507.371 51	95.074	3.069	26.265
5R	-415.358 43	83.650	2.031	23.709
5P	-491.382 32	102.768	3.136	26.327
6R	-463.281 05	59.811	1.829	23.387
6P	-539.316 01	79.010	2.934	25.951
7R	-431.338 24	75.737	1.941	23.561
7P	-507.360 38	94.797	3.048	26.157
8R	-431.714 05	84.917	2.029	23.715
8P	-507.756 01	103.871	3.268	26.689
9aR	-486.380 55	86.365	2.915	25.802
9aP	-562.403 25	105.216	3.824	27.825
9bR	-486.380 55	86.365	2.915	25.802
9bP	-562.412 81	105.502	4.100	28.947
10aR	-782.943 69	71.629	3.975	28.782
10aP	-858.980 10	90.308	4.993	30.872
10bR	-782.943 69	71.629	3.975	28.782
10bP	-858.978 28	90.808	5.096	31.525
11R	-448.514 77	83.221	2.682	25.746
11P	-524.526 82	102.216	3.907	28.323
12R	-464.457 80	75.125	2.609	25.500
12P	-540.480 50	94.322	3.783	28.097
13R	-464.429 70	74.560	2.633	25.482
13P	-540.450 06	94.003	3.792	27.935
14R	-432.512 19	90.826	2.683	25.222
14P	-508.516 04	109.582	3.933	27.953
15R	-432.512 11	90.737	2.759	25.651
15P	-508.524 96	109.914	3.871	28.281
16R	-784.128 25	86.750	4.847	31.678
16P	-860.149 68	105.567	5.898	33.147
17R	-547.371 14	78.064	3.159	27.020
17P	-623.398 17	96.829	4.231	29.085
18R	-547.375 27	77.898	3.147	27.348
18P	-623.388 09	96.930	4.368	29.488
19R	-547.368 01	78.025	3.147	26.723
19P	-623.378 30	97.061	4.388	29.479
20R	-376.604 76	74.136	2.199	23.833
20P	-452.647 50	93.339	3.396	27.165
21R	-475.440 71	68.668	2.722	25.219
21P	-551.487 29	88.020	3.895	28.197

^a Units are in Hartrees. ^b Units are in kcal/mol at $T = 298$ K. R = reactant. P = product (hydrate).

two molecules (S1 and S2) was computed using eq 6

$$\Delta G_3 - \Delta G_1 = \Delta G_{\text{aq}} - \Delta G_{\text{gas}} = \Delta \Delta G_{\text{sol}} \quad (6)$$

The relative binding free energy change for the two molecules was computed using eq 7

$$\Delta G_4 - \Delta G_2 = \Delta G_{\text{com}} - \Delta G_{\text{aq}} = -k_{\text{B}}T \ln(k_2/k_1) = \Delta \Delta G_{\text{bind}} \quad (7)$$

where ΔG_{com} and ΔG_{aq} are the free energy differences for the two molecules in the complex and solvent, respectively, k_{B} is the Boltzmann constant, T is the absolute temperature, and k_1 and k_2 are the binding constants for S1 and S2, respectively. Free energies were calculated in solvent and in the complex for both the mutation of HPR to (6R)-6-hydroxy-1,6-dihydro-8-azapurine riboside (8-aza-HPR) and the reverse. Results in each phase of the simulation are the average of four calculations, i.e., forward and reverse mutations starting with HPR and 8-aza-HPR. Error bars are estimated for each window by dividing the window statistics into four groups and computing the

standard deviation. The root-mean-square of these window errors is reported as a measure of the statistical uncertainty in the results for each complete mutation.

Resonance Energies. Bond separation energies for benzene, 9-methylpurine, 8-aza-9-methylpurine, 2-aza-9-methylpurine, and pteridine and their corresponding hydrates were determined using energies calculated for all molecules of the corresponding isodesmic reaction.¹⁹ Global minimum energies for each molecule were calculated on fully optimized structures using Gaussian92 at the 6-31G** basis set level. The zero-point vibrational energies for each molecule were calculated using calculated harmonic frequencies. Benzene was included in the set of molecules for comparison to literature values.

Results

The calculated global minimum energies for each heteroaromatic compound (Tables 1 and 2) and its corresponding hydrate are shown in Table 3.

Azanaphthalenes. Hydration free energy differences for 10 azanaphthalenes were calculated and compared to experimental data (Table 4). The ratio of the hydrated neutral species to the anhydrous neutral species is reported for 1,3,5,8-tetraazanaphthalene (**1**, pteridine),^{20a} 1,3,8-triazanaphthalene (**2**),^{20b} 1,3,5-triazanaphthalene (**3**),^{20b} 1,3,7-triazanaphthalene (**4**),^{20c} and 1,3-diazanaphthalene (**5**)^{20b} to be 2.9×10^{-1} , 2.0×10^{-3} , 4.5×10^{-3} , 2.0×10^{-2} , and 5.5×10^{-5} , respectively. Conversion of these data to hydration free energy differences relative to pteridine for compounds **2–5** gave results in good agreement with the calculated results. Similarly, the $\Delta \Delta G_{\text{hyd}}$ of -6.1 kcal/mol for 7-azapteridine (**6**) relative to pteridine correctly predicted the experimental observation, i.e., that **6** is completely hydrated^{7a,21} under conditions in which pteridine (**1**) is approximately 20% hydrated.²²

The extent of hydration is also reported to be dependent on both the ionic state of the molecule as well as on the substituents attached to the heteroaromatic ring. For example, 1,4,6-triazanaphthalene (**7**) is poorly hydrated as the neutral species (1.0×10^{-4}), whereas the protonated species (**8**) has a ratio of hydrated species to anhydrous species of 95.²³ The corresponding hydration free energy difference of 8.2 kcal/mol is qualitatively similar to the calculated value of 10.9 kcal/mol and supportive of the experimental finding that the protonated molecule is strongly hydrated relative to the neutral species. Similar success was achieved in calculations of substituted azanaphthalenes. In specific, pteridines substituted at C4 with either methyl (**9**) or trifluoromethyl (**10**) were studied (Scheme 2). Experimentally 4-trifluoromethylpteridine (**10**) is completely hydrated under conditions that produce approximately 20% of the 3,4-double bond hydrate of pteridine²⁴ and no detectable hydrate of 4-methylpteridine (**9**).^{7a,20a,20c} As shown in Table

(19) Roberiro da Silva, M. A. V.; Matos, M. A. R.; Morais, V. M. F. *J. Chem. Soc., Faraday Trans.* **1995**, 91, 1907–1910.

(20) (a) Perrin, D. D. *J. Chem. Soc.* **1962**, 645–653. (b) Armarego, W. L. F. *J. Chem. Soc.* **1962**, 4094–4103. (c) Albert, A. *Angew. Chem., Int. Ed. Engl.* **1967**, 6, 919–928.

(21) Compounds reported to be “completely hydrated” were arbitrarily assumed to hydrate 99.99% based on results for related compounds which were analyzed using the same experimental methods and quantitatively measured to hydrate 99.9%.^{7c} Accordingly, the experimental relative hydration free energies were calculated using the equation $\Delta \Delta G_{\text{hyd}} = -RT \ln(\alpha_1/\alpha_2)$ where α_1 and α_2 are the ratios of the hydrated species to the anhydrous species for compound **1** and compound **2**, respectively. If compound **1** is completely hydrated, then α_1 is 9999.

(22) Biffin, N. E. C.; Brown, D. J.; Sugimoto, T. *J. Chem. Soc. C.* **1970**, 139–145.

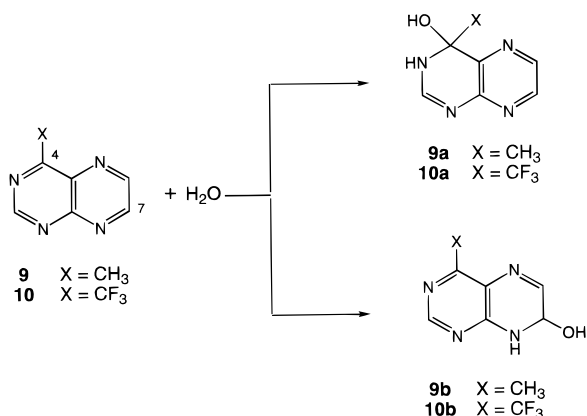
(23) Perrin, D. D.; Inoue, Y. *J. Phys. Chem.* **1962**, 66, 1689.

(24) Clark, J.; Pendergast, W. *J. Chem. Soc. C.* **1969**, 1751–1754.

Table 4. Relative Hydration Free Energy Differences for Azanaphthalenes^a

comps	$\Delta\Delta H_{\text{gas}}^b$	$T\Delta\Delta S_{\text{gas}}$	$\Delta\Delta G_{\text{gas}}$	$\Delta\Delta\Delta G_{\text{sol}}^c$	$\Delta\Delta G_{\text{hyd}}^{\text{(calc)}}$	$\Delta\Delta G_{\text{hyd}}^{\text{(expt) } d}$
1 – 2	-1.372	-0.070	-1.302	-1.3	-2.6	-2.9
1 – 3	-0.797	-0.006	-0.791	-1.2	-2.0	-2.5
1 – 4	-0.009	-0.101	0.092	-1.3	-1.2	-1.6
1 – 5	-2.308	-0.066	-2.242	-1.8	-4.0	-5.1
1 – 6	4.558	-0.012	4.570	1.5	6.1	6.2 ^e
3 – 5	-1.511	-0.060	-1.451	-0.6	-2.1	-2.6
7 – 8	12.410	-0.378	12.788	-1.9	10.9	8.2
9b – 9a	-5.437	1.122	-6.559	0.7	-5.9	
10a – 9b	-3.229	-1.055	-2.174	-1.0	-3.2	
10b – 10a	1.745	0.653	1.092	0.8	1.9	
1 – 10a	6.075	0.462	5.613	-0.2	5.4	6.2 ^e
5 – 10a	8.382	0.528	7.854	1.5	9.4	11.3 ^e
3 – 10a	6.872	0.468	6.404	1.1	7.5	8.7 ^e

^a Units are in kcal/mol. ^b $\Delta\Delta E(\text{HF}) + \Delta\Delta E(0) + \Delta\Delta\Delta E(\text{v})$. ^c Standard errors ranged from ± 0.4 – 0.5 kcal/mol. ^d References for the ratios of hydrated species to anhydrous species for each compound are reported in text. ^e Reference 21.

Scheme 2

4, the relative hydration free energy difference for **10a** and **1** is 5.4 kcal/mol, which is qualitatively similar to the lower limit of 6.2 kcal/mol estimated from the experimental data and based on the detection limits reported for the analytical methodology.^{7a} The calculated results also correctly predicted the large difference in hydration between the methyl (**9a**) and trifluoromethyl (**10a**) pteridine analogues (≈ 9 kcal/mol). In this case, only a lower limit could be estimated, since **9** does not form measurable quantities of the 3,4-double bond hydrate but rather forms a small percent of the 5,6–7,8-dihydrate as the protonated species.^{7a}

The relative hydration free energy differences for the 7,8-double bond hydrates of both **9** and **10** were calculated in order to assess whether the dependence of the hydration site on the substituent at C4 could accurately be predicted. As shown in Table 4, the calculated results support the hydration site preference observed experimentally in that the $\Delta\Delta G_{\text{hyd}}$ for the 3,4-double bond hydrate and 7,8-double bond hydrate for 4-methylpteridine (**9**) is 5.9 kcal/mol, whereas it is -1.9 kcal/mol for 4-trifluoromethylpteridine (**10**). The modest preference for the 3,4-double bond hydrate for **10** is consistent with the experimental observation that in aqueous solutions **10** is reported to first form the 5,6–7,8-dihydrate which then equilibrates over time to the more stable 3,4-double bond hydrate.^{7a}

Purines. Purine riboside is predicted to hydrate across the N1–C6 double bond to an extremely limited extent in aqueous solutions based on the equilibrium constant ($K_{\text{eq}} = 1.1 \times 10^{-7}$) estimated from spectroscopic studies conducted on 1-methylpurinium ribonucleoside cation.²⁵ In an effort to identify purine

Table 5. Relative Hydration Free Energy Differences for Purine Analogs^a

comps	$\Delta\Delta H_{\text{gas}}^b$	$T\Delta\Delta S_{\text{gas}}$	$\Delta\Delta G_{\text{gas}}$	$\Delta\Delta\Delta G_{\text{sol}}^c$	$\Delta\Delta G_{\text{hyd}}^{\text{(calc)}}$
11 – 12	6.532	-0.020	6.552	0.5	7.1
11 – 13	4.832	0.124	4.708	0.4	5.1
11 – 14	-4.932	-0.154	-4.778	-0.5	-5.3
11 – 15	0.433	-0.053	0.486	-0.6	-0.1
11 – 16	6.238	1.108	5.130	-0.4	4.7
11 – 17	9.783	0.512	9.271	-0.8	8.5
11 – 18	0.451	0.437	0.014	-0.5	-0.5
11 – 19	-1.161	-0.179	-0.982	-0.4	-1.4

^a Units are in kcal/mol. ^b $\Delta\Delta E(\text{HF}) + \Delta\Delta E(0) + \Delta\Delta\Delta E(\text{v})$. ^c Standard errors ranged from ± 0.3 – 0.5 kcal/mol.

analogues with more favorable hydration equilibria, the effect of purine ring atoms and ring substituents on the extent of purine hydration was studied. Since the ribose was not expected to significantly affect hydration of the purine base, the ribose was replaced with methyl in the relative hydration free energy difference calculations. From the results shown in Table 5, electron withdrawing groups at C6, e.g., fluoro (**17**) or trifluoromethyl (**16**), produce the largest enhancement in hydration, which is reminiscent of results found for carbonyl-containing compounds.⁶ The order of hydration was predicted for 9-methylpurine analogues to be 6-fluoropurine (**17**) > 6-trifluoromethylpurine (**16**) > purine (**11**) > 2-fluoropurine (**18**) > 8-fluoropurine (**19**). In addition to substituted purines, a set of aza and deaza 9-methylpurine analogues was evaluated. Results shown in Table 5 indicate that the order of hydration is 8-azapurine (**12**) > 2-azapurine (**13**) \gg purine (**11**) > 7-deazapurine (**15**) \gg 3-deazapurine (**14**). Hence, the extent of hydration is decreased by the deletion of heteroatoms in the purine ring and increased by the addition of heteroatoms.

The calculated hydration free energies indicate that the addition of a nitrogen at the 8-position (i.e., 8-aza-9-methylpurine **12**) enhances hydration to the largest extent, i.e., 7.1 kcal/mol more favorable than 9-methylpurine. Experimentally the hydrate of 8-azapurine riboside is undetectable in solution,²⁶ which is consistent with the calculated result, despite the large $\Delta\Delta G_{\text{hyd}}$, since 9-methylpurine, like purine riboside, is likely to have a highly unfavorable equilibrium constant ($K_{\text{eq}} = 10^{-7}$) and therefore exists as the hydrate less than 0.2%.

The relative hydration free energy was also calculated for pteridine and 9-methylpurine in order to assess the accuracy of the calculations with two molecules of greater structural dissimilarity. The calculated result (**1**–**11**, -9.3 kcal/mol) was

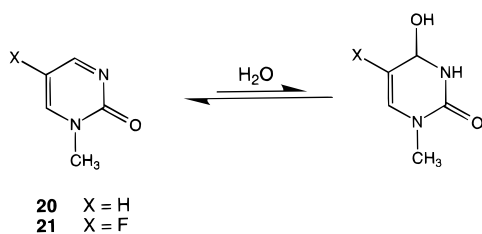
(25) Jones, W.; Wolfenden, R. *J. Am. Chem. Soc.* **1986**, *108*, 7444–7445.

(26) (a) Albert, A. *J. Chem. Soc. C* **1966**, 427–433. (b) Bunning, J. W.; Perrin, D. D. *J. Chem. Soc. C* **1966**, 433–436. (c) Albert, A. *J. Chem. Soc. B* **1966**, 438–441.

compd	Bond Separation Reaction		
Benzene	Benzene	+ 6CH ₄	→ 3CH ₃ CH ₃ + 3CH ₂ CH ₂
11	11	+ 5NH ₃ + 7CH ₄	→ 3CH ₂ NH + C ₂ H ₄ + 6CH ₃ NH ₂ + CH ₃ CH ₃
11 •H ₂ O	11 •H ₂ O	+ 5NH ₃ + 8CH ₄	→ 2CH ₂ NH + C ₂ H ₄ + 7CH ₃ NH ₂ + CH ₃ CH ₃ + CH ₃ OH
12	12	+ 6NH ₃ + 6CH ₄	→ 2CH ₂ NH + C ₂ H ₄ + N ₂ H ₂ + 5CH ₃ NH ₂ + CH ₃ CH ₃ + N ₂ H ₄
12 •H ₂ O	12 •H ₂ O	+ 6NH ₃ + 7CH ₄	→ CH ₂ NH + C ₂ H ₄ + N ₂ H ₂ + 6CH ₃ NH ₂ + CH ₃ CH ₃ + N ₂ H ₄ + CH ₃ OH
13	13	+ 6NH ₃ + 6CH ₄	→ 2CH ₂ NH + C ₂ H ₄ + N ₂ H ₂ + 5CH ₃ NH ₂ + CH ₃ CH ₃ + N ₂ H ₄
13 •H ₂ O	13 •H ₂ O	+ 6NH ₃ + 7CH ₄	→ CH ₂ NH + C ₂ H ₄ + N ₂ H ₂ + 6CH ₃ NH ₂ + CH ₃ CH ₃ + N ₂ H ₄ + CH ₃ OH
1	1	+ 4NH ₃ + 8CH ₄	→ 4CH ₂ NH + 4CH ₃ NH ₂ + C ₂ H ₄ + 2CH ₃ CH ₃
1 •H ₂ O	1 •H ₂ O	+ 4NH ₃ + 9CH ₄	→ 3CH ₂ NH + 5CH ₃ NH ₂ + C ₂ H ₄ + 2CH ₃ CH ₃ + CH ₃ OH

Figure 1. Bond separation reactions for benzene and compounds **1**, **11**, **12**, and **13** and their corresponding hydrates.

Scheme 3



similar to the experimental value estimated for pteridine (**1**) and purine riboside (−8.8 kcal/mol).^{20a,25}

Pyrimidines. Simple pyrimidin-2-ones are reported to hydrate approximately 0.1–1% in aqueous solution (Scheme 3).²⁷ Zebularin, 2-(1*H*)-pyrimidinone riboside, inhibits cytidine deaminase (CDA) with a $K_i(\text{app}) = 10 \mu\text{M}$,^{28a} whereas the 5-fluoro analogue inhibits CDA with a $K_i(\text{app}) = 1 \mu\text{M}$.^{28b} Similar to studies on purine riboside, the hydration free energy difference for the corresponding 1-methyl analogues was calculated and shown to favor the 5-fluoro analogue **21** over the unsubstituted analogue **20** by 1.6 kcal/mol.

Tautomer Energies. Gas-phase quantum mechanical free energies were calculated for the N3(H) tautomer of purine, the N1(H) and N8(H) tautomers of pteridine, the N3(H) tautomer of 7-deaza-9-methylpurine, and the enol tautomer of pyrimidin-2-one. In all but the N1(H) tautomer of pteridine, energies for the geometry optimized structures were greater than 12 kcal/mol higher than the tautomers shown above. These results are consistent with previous experimental and theoretical studies on purine tautomerism.²⁹ The relative solvation free energy was calculated^{29d} for the N1(H) and N3(H) tautomers of pteridine since their gas-phase free energies differed by only 1.4 kcal/

(27) Katritzky, A. R.; Kingsland, M.; Tee, O. S. *J. Chem. Commun.* **1968**, 289–290.

(28) (a) McCormack, J. J.; Marquez, V. E.; Liu, P. S.; Vistica, D. T.; Driscoll, J. S. *Biochem. Pharmacol.* **1980**, *29*, 830–832. (b) Driscoll, J. S.; Marquez, V. E.; Plowman, J.; Liu, P. S.; Kelly, J. A.; Barchi, Jr., J. J. *J. Med. Chem.* **1991**, *34*, 3280–3284.

(29) (a) Pullman, B.; Pullman, A. *Adv. Heterocycl. Chem.* **1971**, *13*, 77. (b) Chenon, M.-T.; Pugmire, R. J.; Grant, D. M.; Panzica, R. P.; Townsend, L. B. *J. Am. Chem. Soc.* **1975**, *97*, 4627–4642. (c) Erion, M. D.; Stoeckler, J. D.; Guida, W. C.; Walter, R. L.; Ealick, S. E. *Biochemistry* **1997**, *36*, 11735–11748.

Table 6. Calculated Bond Separation Energies (kcal/mol)

	$\Delta E(\text{HF})$	$\Delta E(0)$	$\Delta E(\text{HF}) + \Delta E(0)$
benzene	58.23	5.92	64.15
9-methylpurine (11)	118.63	15.97	134.60
11 •H ₂ O	107.64	17.53	125.17
$\Delta\Delta E^a$	−10.99	1.56	−9.43
8-aza-9-methylpurine (12)	124.70	16.39	141.09
12 •H ₂ O	120.44	17.86	138.30
$\Delta\Delta E^a$	−4.26	1.47	−2.79
2-aza-9-methylpurine (13)	107.07	16.96	124.03
13 •H ₂ O	101.46	18.11	119.57
$\Delta\Delta E^a$	−5.61	1.15	−4.46
pteridine (1)	115.32	15.26	130.58
1 •H ₂ O	112.99	17.01	130.00
$\Delta\Delta E^a$	−2.33	1.75	−0.58

^a Resonance energy difference (hydrate − anhydrous).

mol. The results indicate that in solution the N3(H) pteridine tautomer is further stabilized and based on the sum of the free energies is favored over the N1(H) tautomer by 1.9 kcal/mol.

Resonance Energies. Resonance energies were calculated for the anhydrous and hydrated forms of four heteroaromatic compounds. Results obtained using the indicated isodesmic reactions (Figure 1) are shown in Table 6 and indicate that hydration of 9-methylpurine (**11**) results in a large decrease in resonance energy (>9 kcal/mol), whereas only a small decrease is found for pteridine (**1**) and its hydrate. Analysis of two purine analogues suspected to hydrate considerably more than purine itself, namely 8-aza-9-methylpurine (**12**) and 2-aza-9-methylpurine (**13**), show that both compounds lose considerably less resonance energy upon hydration compared to 9-methylpurine (**11**).

Adenosine Deaminase Binding Affinity. The average structure for the ADA–HPR complex generated after energy minimization and equilibration with 20 ps of MD simulation showed considerable movement of atoms in the vicinity of the zinc ion when these residues were not constrained. After constraints were applied, however, the average structure was

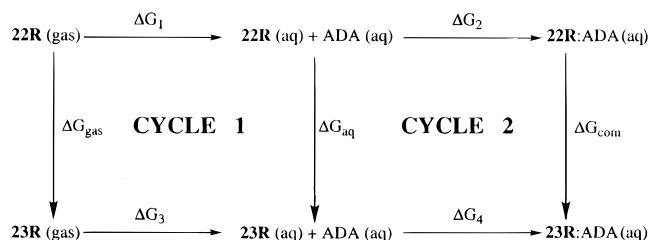


Figure 2. Thermodynamic cycles used to calculate the relative binding free energy (cycle 2) and relative solvation free energy (cycle 1) for the 6*R*-stereoisomer of the 1,6-double bond hydrates of purine riboside (**22R**) and 8-azapurine riboside (**23R**). $\Delta\Delta G_{\text{sol}} = \Delta G_{\text{aq}} - \Delta G_{\text{gas}} = -1.1 \pm 0.5$ kcal/mol and $\Delta\Delta G_{\text{bind}} = \Delta G_{\text{com}} - \Delta G_{\text{aq}} = 3.1 \pm 0.7$ kcal/mol (**23R**–**22R**).

similar to the X-ray structure with root-mean-square deviations of less than 1.0 Å for backbone atoms and 1.45 Å for side chain atoms.

Using this structure and the TCP method, the relative binding free energy for HPR (**22R**) and its 8-aza analogue (**23R**) was calculated (Figure 2, Cycle 2). The results indicate that **23R** has a 190-fold lower intrinsic binding affinity relative to **22R** ($\Delta\Delta G_{\text{bind}} = 3.1 \pm 0.7$ kcal/mol). The decreased binding affinity is attributed in part to a 1.1 ± 0.5 kcal/mol increase in desolvation energy for the 8-aza analogue as calculated from the gas phase and solvent phase free energies (Figure 2, Cycle 1).

Discussion

Using methodology previously applied to carbonyl-containing compounds,⁶ relative hydration free energy differences for a variety of structurally diverse heteroaromatic compounds were calculated and the results compared to experimental data. As indicated in Table 4, both gas-phase quantum mechanical energy ($\Delta\Delta G_{\text{gas}}$) and solvation free energy ($\Delta\Delta G_{\text{sol}}$) differences contributed to the final relative hydration free energy difference. Good agreement with experimental data was achieved across a set of compounds exhibiting a wide range of hydration equilibrium constants (10^{-6} – 10^3). Furthermore, good agreement was achieved without including electron correlation contributions in the calculation of $\Delta\Delta G_{\text{gas}}$. The accuracy of these results is attributed in part to the cancellation of systematic errors which arise in the gas phase quantum mechanical free energy and in the solvation free energy calculations but are canceled when calculating the difference between two hydration reactions involving structurally similar molecules. For example, errors in the free energy contribution of the water molecule completely cancel when calculating relative differences since the water molecule is common to both reactions. Furthermore, calculation of relative solvation free energies avoids the large structural perturbation between sp^2 and sp^3 hybridized molecules present in the absolute free energy calculations and therefore errors arising from poorly converged calculations.⁶

Results from a variety of studies indicate that hydration of heteroaromatic compounds is highly dependent on the presence and position of heteroatoms in the ring, their protonation state, and the position and nature of the substituents attached to the ring. Some of the molecular factors that control the hydration reaction are similar to factors previously identified in theoretical studies on carbonyl-containing compounds, which as recently reported by Wiberg included inductive effects that stabilize or destabilize the unhydrated species, ring strain, and bond eclipsing.^{5a} For example, the dependence of the hydration reaction on the electronic and steric nature of substituents located

at the site of hydration is common to both carbonyl-containing compounds and heteroaromatic compounds. In both cases, electron withdrawing groups enhance hydration, whereas electron donating and sterically bulky groups diminish hydration. Accordingly, 1,1,1-trifluoromethylacetone is known to be completely hydrated in aqueous solution, whereas acetone is only about 0.1% hydrated.⁴ Similarly, experimental data for pteridine analogues show that 4-trifluoromethylpteridine (**10**) exists as the hydrate in aqueous solution, whereas pteridine is only partially hydrated ($\approx 20\%$) and 4-methylpteridine (**9**) shows no measurable hydrate. In fact, **9** hydrates only as the protonated species and only across the 5,6–7,8-double bonds to form the corresponding dihydrate.²⁴ As was previously shown for carbonyl-containing compounds,⁶ the combined use of ab initio quantum mechanical calculations and free energy perturbation methods accurately predict the effect of these substituents on heteroaromatic hydration. These calculations indicate that the difference in hydration between the methyl- and trifluoromethylpteridine analogues is approximately 9 kcal/mol, which is similar to the 7 kcal/mol difference reported for trifluoromethylacetone and acetone.⁶ Furthermore, hydration free energy differences between the 3,4-hydrate and the 7,8-hydrate were calculated for both analogues and the results shown to accurately predict the dependence of the preferred hydration site on the substituent at C4.

In addition to ring substituents located at the site of hydration, heteroaromatic compound hydration is affected by substituents located at other ring positions as well as by the ring atoms and the type of aromatic ring. For example, protonation of 1,4,6-triazanaphthalene (**7**), which is known to occur exclusively on the pyridyl nitrogen, is reported to have a dramatic effect on the hydration equilibrium with the neutral molecule existing predominantly in the anhydrous form and the protonated species (**8**) existing as the hydrate.²³ The enhanced hydration of the 1,2-double bond is likely to result from the increased contribution of the quinonoidal resonance structure (4-aminopyridine-type resonance).^{7b} Calculation of the relative hydration free energy difference between the unprotonated and protonated forms of 1,4,6-triazanaphthalene gave a $\Delta\Delta G_{\text{hyd}} = 10.9$ kcal/mol, which is consistent with the qualitative data reported in the literature. Other examples are described in the literature that implicate both ring substituents and ring atoms in resonance stabilization or destabilization of the unhydrated species.⁷ These results indicate that heteroaromatic hydration is frequently more complex than carbonyl hydration since inductive effects can be transmitted through aromatic π -systems.

These factors alone, however, fail to explain several well-known examples of heteroaromatic hydration. In particular, the 10^7 -fold rightward shift in the hydration equilibrium for pteridine (**1**) relative to purine riboside (**24**). This shift is not readily explained by the presence of the ribose in **24** given the low likelihood that the 9-substituent influences the hydration reaction and given the lack of detectable quantities of the hydrated species generated from purine^{7b} as well as several purine analogues^{26c} in both neutral and acidic solutions. Furthermore, the close structural similarity between the heteroaromatic ring systems makes it unlikely that differences in electronic and steric effects can account for the large difference in hydration. In fact, no structural differences are found in the pyrimidine ring or near the hydration site, i.e., the 1,6-double bond of the pyrimidine ring. Thus, the only structural difference between the pteridine and purine ring system is in the ring fused to the pyrimidine ring, which differs by a single aromatic carbon atom not even directly bonded to the pyrimidine ring. For similar

reasons, steric and electronic effects are also not expected to produce a large difference in product stability. A small difference, however, cannot be ruled out, especially given that an intramolecular hydrogen bond can form between the hydroxyl and either the pyrazine or imidazole ring nitrogen. A large difference in the strength of this hydrogen bond is unlikely, however, based on the relative basicities of each nitrogen.

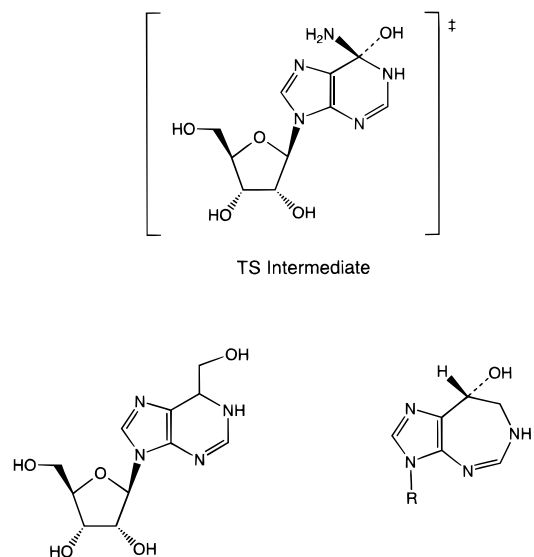
One factor that could account for the large difference between purine and pteridine hydration is the relative loss in aromaticity accompanying hydration of a heteroaromatic ring as indicated by the difference in resonance energy between the anhydrous species and hydrated product. Strong support for aromaticity as a key factor is evident from the resonance energies calculated for pteridine and 9-methylpurine (**11**) using the corresponding isodesmic reactions (Figure 1). As shown in Table 6, hydration of 9-methylpurine results in a 9.4 kcal/mol loss in resonance energy, whereas pteridine loses only 0.6 kcal/mol. This 8.8 kcal/mol difference readily accounts for the free energy difference in hydration of purine relative to pteridine ($\Delta\Delta G_{\text{hyd}}$ (calc) = 9.3 kcal/mol; $\Delta\Delta G_{\text{hyd}}$ (exp) \approx 8.8 kcal/mol). Analogously, analysis of the resonance energy lost upon the hydration of 8-aza- and 2-aza-9-methylpurine suggests that these analogues should also exhibit increased hydration relative to the corresponding purine analogue. Indeed, the difference in resonance energy lost between 8-aza-9-methylpurine (**12**) and 9-methylpurine (**11**) is 6.6 kcal/mol, which is similar to the hydration free energy difference of 7.1 kcal/mol. Similarly, the difference in resonance energy for 2-aza-9-methylpurine (**13**) and 9-methylpurine is 5.0 kcal/mol, which is again very close to the calculated hydration free energy difference of 5.1 kcal/mol. These results strongly support differences in aromaticity as a key factor in heteroaromatic hydration.

Design of Enzyme Inhibitors

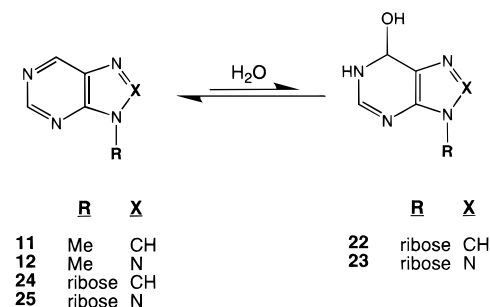
Interest in heteroaromatic hydration stems in part from the realization that covalent hydration can produce hydrated species which potently inhibit certain enzymes, especially enzymes that catalyze reactions involving hydration and hydrated molecules in the transition state (TS). Enzymes of particular interest to us are the deaminases that catalyze the hydration of a $\text{N}=\text{C}-\text{NH}_2$ heteroaromatic double bond, since many of these enzymes represent potential drug targets. For example, inhibitors of adenosine deaminase (ADA),³⁰ which catalyzes the hydration of a purine ring during the conversion of adenosine to inosine and cytidine deaminase (CDA),³¹ which catalyzes the hydration of a pyrimidine ring during the conversion of cytidine to uridine, are reported to have substantial therapeutic potential for treatment of cardiovascular disease and cancer.

Efforts to design potent and specific inhibitors of deaminases have focused on molecules that mimic the TS structure. Since the TS structure most likely resembles the hydrated intermediate, stable TS mimics containing a hydroxyl group attached to a tetrahedral carbon located in a position analogous to the purine hydration site were designed (Scheme 4).³² Alternatively, substrate analogues that undergo reversible covalent hydration may represent an even better strategy since the hydrated product has higher structural similarity to the TS structure and therefore would be expected to exhibit greater potency and specificity.³³

Scheme 4



Scheme 5



Two examples are reported in the literature that unambiguously demonstrate the involvement of the hydrated species in the inhibition of deaminases and the potential power of substrate analogues as deaminase inhibitors. In one example, purine riboside, which is the desamino analogue of adenosine, was shown by both spectroscopic studies³⁴ and by an X-ray crystallography¹⁴ to exist as the 1,6-double bond hydrate (i.e., HPR, **22R**) in the ADA-inhibitor complex. In the other example, the 3,4-double bond hydrate of a desamino analogue of cytidine was identified as the inhibitor of CDA by X-ray crystallography.³⁵ The presence of the hydrated species in these binding sites under conditions that produced no detectable quantities of the hydrated form in aqueous solution ($\ll 1\%$) suggests that the hydrated species may be associated with extraordinarily high enzyme binding affinities. In the case of purine riboside, the hydration equilibrium constant was estimated to be about 10^{-7} using model reactions.^{36a} The inhibitory constant for the hydrated species was therefore calculated to be a remarkable 10^{-13} M^{36b,c} based on the apparent inhibitory constant of purine riboside (10^{-6} M)^{36c} and the mathematical relationship that relates each parameter, i.e., $K_i(\text{app}) = K_i^*(1 + 1/K_{\text{eq}}) \approx K_i^*/K_{\text{eq}}$.

(33) Wolfenden, R. *Acc. Chem. Res.* **1972**, *5*, 10–18.

(34) Kurz, L. C.; Frieden, C. *Biochemistry* **1987**, *26*, 8450–8457.

(35) (a) Betts, L.; Xiang, S.; Short, S. A.; Wolfenden, R.; Carter, C. W. *J. Mol. Biol.* **1994**, *235*, 635–656. (b) Xiang, S.; Short, S. A.; Wolfenden, R.; Carter, C. W., Jr. *Biochemistry* **1995**, *34*, 4516–4523.

(36) (a) The equilibrium constant represents the value obtained using the convention for dilute aqueous solution that treats water as unity. (b) The true K_i^* is half this value since only the *R*-stereoisomer is active. (c) The value of K_i^* is dependent on the value for the apparent inhibitor constant which is reported as 2.9×10^{-6} M by Jones et al.¹⁰ and as 1.6×10^{-5} M by Shewach et al.³⁷

(30) Agarwal, R. P. *Pharmac. Ther.* **1982**, *17*, 399–429.

(31) Marquez, V. E. *Developments in Cancer Chemotherapy*; Glazer, R. I., Ed.; CRC: Boca Raton, FL, 1984; pp 91–114.

(32) (a) Erion, M. D.; Bookser, B. C.; Kasibhatla, S. R. U.S. Patent 5,731,432. (b) Marrone, T. J.; Straatsma, T. P.; Briggs, J. M.; Wilson, D. K.; Quiocho, F. A.; McCammon, J. A. *J. Med. Chem.* **1996**, *39*, 277–284. (c) Evans, B.; Wolfenden, R. *J. Am. Chem. Soc.* **1970**, *92*, 4751.

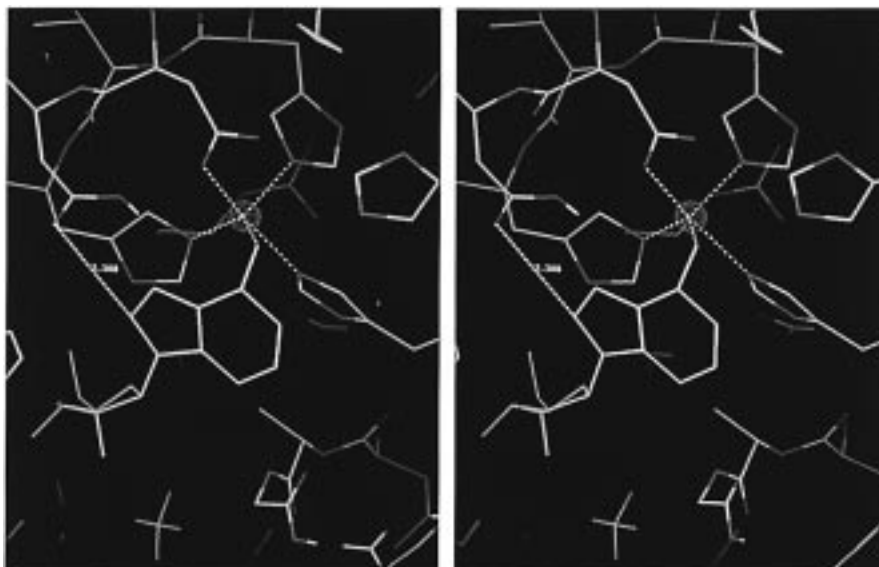


Figure 3. Stereoview of the murine adenosine deaminase active site and (6*R*)-6-hydroxy-1,6-dihydro-8-azapurine riboside (**23R**, yellow) after energy minimization (see Methods). Purple sphere represents the zinc ion which is coordinated with the side chain imidazole groups of His15, His17, and His214, the side chain carboxylate of Asp295 and the 6-hydroxy of **23R**.

The highly unfavorable equilibrium constant exhibited by purine riboside suggests that its rather modest inhibition of ADA ($K_i(\text{app})$) could be significantly enhanced if structural modifications were identified that enhance hydration without decreasing the binding affinity of the hydrated species. Our calculation of relative hydration free energies for pteridine analogues showed that hydration was profoundly affected by modifications in the position or number of heteroatoms in the ring, the substituents attached to the ring as well as the structure of the fused-ring system itself. Similarly, our analysis of purine analogues showed that the ease of hydration for the ring modified 9-methylpurine analogues favored analogues with the greatest number of ring nitrogens, i.e., 8-azapurine (**12**) > 2-azapurine (**13**) \gg purine (**11**) > 7-deazapurine (**15**) > 3-deazapurine (**14**) (Table 5). This trend is attributed to the reduced aromatic character of nitrogen rich heteroaromatic compounds as is further supported by calculation of bond separation energies for 9-methylpurine and its 8- and 2-aza analogues (Table 6). Analysis of substituted 9-methylpurine analogues indicated that electron withdrawing groups at C6 produce a large enhancement in hydration, whereas electron withdrawing groups at the 2- and 8-positions have little or possibly detrimental effects on hydration (Table 5).

To assess whether the modification results in an overall increase in the apparent inhibitory constant, both the relative hydration free energy and the relative binding free energy for the hydrate in the enzyme complex must be calculated. The sum of these free energies is the free energy difference corresponding to the relative change in inhibitory potency, $K_i(\text{app})/K_i'(\text{app})$, as shown in eq 8.

$$\Delta G_{\text{rel}} = -RT \ln(K_i(\text{app})/K_i'(\text{app})) \\ = \Delta\Delta G_{\text{hyd}} + \Delta\Delta G_{\text{bind}} \quad (8)$$

Accordingly, we calculated ΔG_{rel} for purine riboside (**24**, $K_i(\text{app}) = 1.6 \times 10^{-5}$ M) and 8-azapurine riboside (**25**, $K_i(\text{app}) = 4.0 \times 10^{-8}$ M), since this single structural change in purine riboside is reported to increase inhibitory potency 400-fold (Scheme 5).³⁷ The molecular reason for this enhancement in

potency was not determined but could be due to either enhanced hydration of the nucleoside or to increased binding affinity of the hydrated species. Calculation of the relative binding affinity for the hydrated species indicated that the 8-aza analogue **23R** (R denotes the 6*R*-stereochemistry) loses 3.1 ± 0.7 kcal/mol of binding energy thereby eliminating this potential explanation for the 400-fold improvement in ADA inhibitor potency exhibited by **25** (Figure 2). The loss in binding affinity of **23R** is partly attributed to a 1.1 ± 0.5 kcal/mol increase in desolvation energy as calculated using the first thermodynamic cycle (Figure 2). The remaining portion of the lost binding energy, i.e., 2 kcal/mol, likely represents a loss in intrinsic binding affinity which, as observed in the energy minimized ADA complex, may arise from an unfavorable electrostatic interaction between the 8-nitrogen and one of the oxygens in the side chain carboxylate of Asp296 (Figure 3).

The other possible explanation for the 400-fold improvement in inhibitory potency exhibited by 8-azapurine riboside (**25**) may relate to a greater propensity of the 8-aza analogue to hydrate. The relative hydration free energy difference between 9-methylpurine (**11**) and 8-aza-9-methylpurine (**12**) strongly supports this possibility, since the difference is 7.1 kcal/mol or approximately a 5-order of magnitude rightward shift in the equilibrium constant for the 8-aza analogue. The large enhancement in hydration is somewhat surprising, since the hydrated species is not detected in aqueous solution.^{26b} However, given the highly unfavorable equilibrium constant for purine riboside (10^{-7}), the failure to detect the hydrated species may be plausible especially considering that the predicted equilibrium constant would still be on the order of 10^{-2} . Furthermore, studies of other 8-azapurine analogues indicate that the 8-aza substitution has a large effect on hydration. For example, the cation of 8-azapurine and several analogues,^{7c,20c} including the 2-amino-, 2-hydroxy-, 2-mercapto, 7-methyl,^{38a} and 8-methyl^{38b} analogues, are reported to be highly hydrated, whereas purine and purine analogues are not.^{7c} Resonance energy differences for 9-methyl-8-azapurine (**12**) and 9-methylpurine (**11**) relative to their corresponding hydrates (Table 6) suggest that hydration results in less loss of resonance energy

(37) Shewach, D. S.; Krawczyk, S. H.; Acevedo, O. L.; Townsend, L. B. *Biochemical Pharmacology* **1992**, *44*, 1697–1700.

(38) (a) Albert, A.; Tratt, K. *J. Chem. Soc. C* **1968**, 344–347. (b) Albert, A. *J. Chem. Soc. C* **1968**, 2076–2083.

for **12** (6.6 kcal/mol) and therefore that differences in aromaticity may be the key factor accounting for the large hydration free energy differences between purine and 8-azapurine analogues.

The calculated results therefore provide a clear explanation for the 400-fold enhancement observed in the inhibitory potency between purine riboside and its 8-aza analogue.³⁷ The relative hydration free energy difference ($\Delta\Delta G_{\text{hyd}} = -7.1$ kcal/mol) indicates that the 8-azapurine analogue hydrates about 160 000-fold greater than the corresponding purine analogue, whereas the hydrated form of the 8-aza analogue loses approximately 190-fold in binding affinity ($\Delta\Delta G_{\text{bind}} = 3.1$ kcal/mol). These results predict that the hydration equilibrium constant for **25** is approximately 1.8×10^{-2} compared to 1.1×10^{-7} for purine riboside (**24**) and that the binding affinity for the hydrate of **25** is 3.4×10^{-10} M compared to 1.8×10^{-12} M for the hydrate of purine riboside.³⁶ The net effect is a 4.0 kcal/mol enhancement in inhibitory potency for the 8-aza analogue which translates to a predicted $K_i(\text{app})$ for 8-azapurine riboside of 1.9×10^{-8} M; a value close to the experimental result of 4.0×10^{-8} M.³⁷

Conclusions

Four major conclusions are revealed by the results of this study.

(1) Relative hydration free energy differences for a variety of heteroaromatic compounds are accurately calculated using a combined quantum mechanical and free energy perturbation approach. Good agreement with experimental data is obtained for heteroaromatic compounds exhibiting a wide range of hydration equilibrium constants (10^{-6} – 10^3).

(2) Heteroaromatic hydration is controlled by a multitude of molecular factors. Similar to hydration of carbonyl-containing compounds, both steric and electronic effects near the site of hydration can dictate the extent of hydration as well as the site of hydration. An additional factor that can dominate the

hydration of heteroaromatic compounds relates to the loss of aromaticity that accompanies hydration of the heteroaromatic ring. In fact, differences in resonance energy losses accounted for the 10^7 -fold greater propensity of pteridine to hydrate relative to its close structural analogue 9-methylpurine ($\Delta\Delta G_{\text{hyd}}(\text{exp}) \approx 8.8$ kcal/mol; $\Delta\Delta G_{\text{hyd}}(\text{calc}) = 9.3$ kcal/mol).

(3) Accurate calculation of relative inhibitor potencies for ADA inhibitors that undergo covalent hydration requires calculation of both the hydration free energy difference as well as the difference in the binding free energy for the hydrated molecules complexed to ADA. The importance of calculating both free energies was demonstrated in a study of purine riboside and its 8-aza analogue. The results showed that the 400-fold greater inhibitor potency for the 8-aza analogue was due to increased hydration since hydration of 8-aza-9-methylpurine was strongly favored over 9-methylpurine ($\Delta\Delta G_{\text{hyd}} = -7.1$ kcal/mol), whereas the relative binding free energy favored the purine analogue ($\Delta\Delta G_{\text{bind}} = 3.1 \pm 0.7$ kcal/mol). The net effect was a 4.0 kcal/mol enhancement in inhibitor potency for the 8-aza analogue which agrees well with the experimental value.

(4) Computational methods that enable accurate calculation of relative hydration free energies and relative binding free energies are useful for the discovery of substrate analogues that act as potent deaminase inhibitors.

Acknowledgment. We would like to thank Ms. Lisa Weston for her assistance in preparing this manuscript.

Supporting Information Available: Lists of final atomic coordinates and CHELPG charges for the structures of compounds **1–21** (anhydrous and hydrated species) following energy optimization at the 6-31G** basis set level (14 pages). See any current masthead page for ordering and Web access instructions.

JA972906J